



Cite this: *Chem. Commun.*, 2025, 61, 6783

Received 22nd March 2025,
Accepted 2nd April 2025

DOI: 10.1039/d5cc01621e

rsc.li/chemcomm

Easy access to a self-assembled glycolipid derived from bhilawanol: a promising anti-cancer drug†

Tohira Banoo,^a Kajal Sandhu,^b S. Chockalingam^{ib} and Subbiah Nagarajan^{ib}*^a

In this study, we synthesised a series of self-assembling glycoconjugates derived from bhilawanol under environmentally friendly conditions in good yields. These self-assembling glycoconjugates displayed anti-cancer activity toward HeLa cells at an IC₅₀ value of 125 μM with minimal side effects, holding immense potential in cancer therapeutics.

Cancer encompasses a range of diseases characterised by uncontrolled cell division and compromised immune system leading to mortality.¹ Despite significant strides in cancer therapeutics and diagnostics, the medical community continues to strive for further advancements in combating this disease.² It has been witnessed that plant extracts have played a predominant role in cancer treatment since ancient times. In this study, we focused on synthesising a class of new glycolipids from a renewable resource, bhilawanol, also known as urushiol, a bioactive molecule obtained from "*Semecarpus anacardium*", found in India's sub-Himalayan, tropical, and central regions, that has been used as a traditional Indian medicine for centuries to treat various ailments.³ The seeds of this plant are reported to contain many biologically active molecules displaying potential anticancer, antibacterial, antifungal, and other biological properties.⁴ Sahoo and co-workers recently presented a mini-review highlighting the potential applications of *Semecarpus anacardium* Linn. (SCA) in anticancer and anti-inflammatory therapies. The review underscores SCA's therapeutic potential in treating various cancers, including breast cancer, lung cancer, blood cancer, and hepatocellular carcinoma, with advancements reaching clinical trials. It also emphasizes the need for further investigation into the use of SCA extracts in cancer treatment.⁵ In this report, the conjugation of carbohydrates with bhilawanol resulted in a new class of biologically active glycolipids. The direct conjugation of bhilawanol to carbohydrates or amino

acids has not been reported to date. Lepoittevin and co-workers have coupled 3-*n*-alkyl catechols to the acetate or trichloroimidates of monosaccharides and disaccharides using multistep synthesis.⁶ Later, in a patent report, amino acids and N-heterocyclic compounds were conjugated to bhilawanol and their biological properties were evaluated.⁶ Carbohydrates are essential molecules that play crucial roles in various biological processes such as cell development, recognition, cell-cell interaction and communication, growth, and energy storage.⁷ Hergenrother and coworkers reported the salient features of glycoconjugates in improved cancer targeting and selectivity.⁸ The tendency of cancer cells to metabolise more sugars than normal cells has been leveraged to target cancer cells using glycoconjugates, which is referred to as the Warburg effect.^{9–11} To date, 14 distinct glucose transporters (GLUT) have been identified based on their structure and sequence; among these, GLUT-1 is the most extensively studied glucose transporter and is widely recognized for its overexpression in cancer cells.¹² Consequently, the other stereoisomers of glucose analogues can be effectively taken up by cancer cells, offering an appealing strategy to broaden the Warburg effect to a broader range of glycoconjugates.^{13,14} Given their importance in anticancer activity, synthesising glycoconjugates or glycolipids, particularly those derived from renewable sources, is of significant interest.¹⁵ Glycolipids are also a key class of amphiphiles prone to self-assembly through non-covalent interactions to furnish the supramolecular architecture, which is fundamental in living organisms, leading to functional structures capable of performing intricate biological functions.¹⁶ Recognising the potential of carbohydrates, we investigated the self-assembly of a series of bhilawanol-based glycolipids. This thoughtful design strategy aims to leverage the stabilising role of carbohydrates in complex architectures and explore their promising applications.

Carbohydrate-based self-assembling systems are integral to the creation of advanced biocompatible materials with versatile functionalities, enabling a wide range of applications.^{17,18} In this report, one of the biologically significant natural compounds, bhilawanol (**1a**), has been chemically modified and conjugated with various monosaccharides to synthesize glycoconjugates (BCG).¹⁹ This process employed a straightforward and environmentally friendly

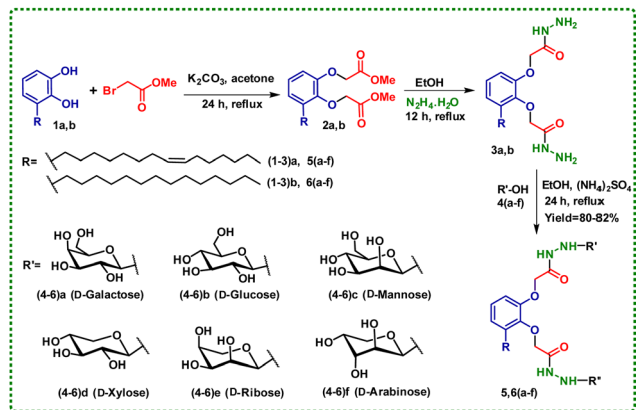
^a Assembled Organic and Hybrid Materials Lab, Department of Chemistry, National Institute of Technology Warangal, Hanumakonda-506004, Telangana, India.

E-mail: snagarajan@nitw.ac.in, snrajannpt@yahoo.co.in

^b Cell Signaling Research Laboratory, Department of Biotechnology, National Institute of Technology Warangal, Hanumakonda-506004, Telangana, India

† Electronic supplementary information (ESI) available. See DOI: <https://doi.org/10.1039/d5cc01621e>



Scheme 1 Synthesis of glycolipids **5,6(a-f)**.

protocol to create glycolipids. The reaction involves treating *phthalan* hydrazide (**3a, b**) with various monosaccharides (**4a-f**) in ethanol, utilising ammonium sulphate as a base under reflux conditions in a single-pot reaction. The established protocol furnished 80–82% of the desired glycolipid without the requirement of column chromatography (Scheme 1).²⁰ The formation of the desired **BCG5,6(a-f)** was confirmed by nuclear magnetic resonance (NMR), high-resolution mass spectrometry (HRMS), and infrared (IR) spectroscopy. The F2-coupled ¹H, ¹³C-HSQC NMR spectrum of **BCG6b** furnished a ¹J_{CH,H} coupling constant of 157 Hz, which is less than 168 Hz, clearly revealing the exclusive formation of the 1,2-*trans*-anomeric product (Fig. S52, ESI†).²¹

Over the past few decades, self-assembling carbohydrates have gained momentum due to their abundance and accessibility. In addition, easy tuning of the orientation of hydroxyl groups, additional functionalisation and hydrogen bonding are the characteristic features.²² This, in turn, has spurred further exploration into the realms of molecular self-assembly and supramolecular chemistry. Low molecular weight gels (LMWGs) were reported as far back as the 19th century, but the scientific understanding of structure and function was not fully elucidated. Notably, in the recent past, researchers have engineered functional molecules and extensively investigated their self-assembly.²² The “stable to inversion” method identified BCGs’ gelation behaviour. Table S1 (ESI†) summarises the gelation capability of BCG glycolipids in different solvents and oils.²³ Interestingly, all the synthesized BCG glycolipids displayed gelation in DMSO. Among the BCG glycolipids **5a-f**, which have unsaturation in their hydrophobic unit, **BCG5a** displays gelation in DMSO + H₂O (40%) with a CGC of 1.5% (wt/v). It is worth mentioning that **BCG6a**, a saturated version of **BCG5a**, exhibited gelation in DMSO + H₂O (40%) with a CGC of 1.0% (wt/v). The better gelation ability of **6a** is attributed to the pronounced molecular stacking displayed by the saturated hydrophobic unit. **BCG5,6(a-f)** show a CGC of 1.0% (wt/v) in linseed oil (Fig. S1, ESI†). The thermal stability of the hydrogel and oleogels formed by **BCG5,6(a-f)** has been identified by the sol-gel transition temperature (*T_g*). Hydrogel and oleogel formed by **BCG5a** and **6a** displayed *T_g* as 117 & 96 °C and 129 & 98 °C, respectively. With an increase in the concentration of the gelator, the *T_g* also increases, indicating the tunability of gel strength, as shown in Fig. S49 (ESI†).

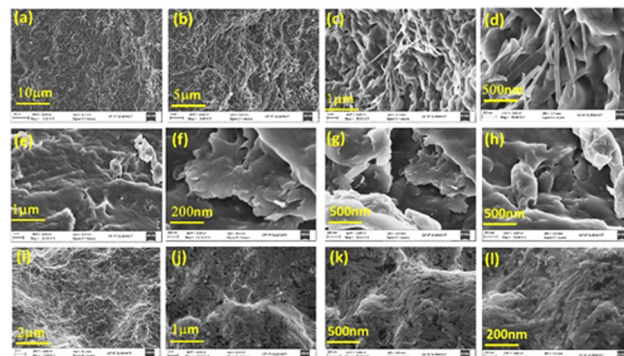


Fig. 1 SEM images of (a)–(d) the hydrogel formed by **BCG6a** in DMSO + H₂O and (e)–(h) the oleogel hydrogel formed by **BCG6a** in linseed oil and (i)–(l) hydrogel formed by **BCG6b** in DMSO + H₂O, respectively.

A scanning electronic microscopy (SEM) analysis of the hydrogel and oleogel formed by **BCG6a** in DMSO + water and Linseed oil and **BCG6b** in DMSO + water was performed to understand the morphology of the gel. The SEM analysis showed that the hydrogel and oleogel formed by **BCG6a** reveal a fibrillar, lamellar-like architecture. In contrast, the hydrogel morphology formed by compound **BCG6b** in DMSO + water reveals a globular structure (Fig. 1). This result clearly demonstrates that the epimers of carbohydrates and the solvent environment both play a crucial role in guiding the supramolecular self-assembly of the gelator into a gel through intermolecular interactions, ultimately influencing its microscopic structure.

Variable temperature NMR (VT-NMR) provides compelling evidence of intermolecular interactions in self-assembly. To our fortune, **BCG6a** forms a hydrogel in DMSO–H₂O, favouring the VT-NMR studies. The VT-NMR spectral studies of the gel displayed a remarkable change compared to the solution state. The disappearance of exchangeable protons and broadening of aromatic signals with minimal shifts is observed (Fig. 2a). In the gel state, a decrease in the intensity of sugar peaks and the disappearance of signals corresponding to aromatic and hydrophobic units is observed. Even up to 60 °C, a similar trend was observed; however, further increase in temperature to 90 °C resulted in well-resolved spectra with the up-field shift of aromatic protons centred at around $\delta = 7.0$ ppm to 6.5 ppm, and protons corresponding to sugar and hydrophobic units were observed. The overall up-field shift of protons of **BCG6a** is the result of an increase in the electron density during the molecular self-assembly *via* hydrogen bonding, π – π interactions and van der Waals interactions (Fig. 2a).

Various intermolecular interactions such as hydrogen bonding, hydrophobic interactions, stacking, anionic– π and cationic– π and van der Waals displayed by a molecule play a crucial role in the assembly mechanism. In this study, we explore correlations between molecular structure and self-assembly behaviour, aiming to uncover the fine distinction of these interactions. To gain a deeper insight into the molecular self-assembly of the hydrogel produced from **BCG6a**, we conducted FTIR studies. The molecular self-assembly brings variations in the intermolecular interaction in the amorphous to assembled state due to the formation of secondary interactions. Fig. 2b illustrates the FTIR spectra of **BCG6a** in amorphous and assembled states. In the IR spectra, peaks centred at 3256, 3300,



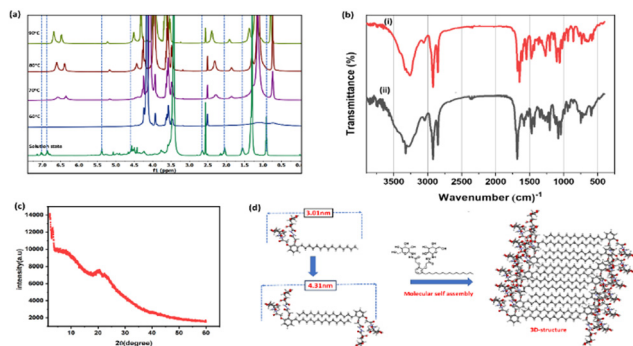


Fig. 2 (a) VT-NMR studies of **BCG6a** hydrogel, (b) FTIR studies of **BCG6a** in the (i) amorphous and (ii) assembled state, (c) SAXRD of the xerogel of **BCG6a**, and (d) proposed bottom-up self-assembly mechanism.

2852, 1680, 1648, 1103 and 1056 cm^{-1} represent the assembled state. In contrast, the amorphous state displayed a shift and was observed at slightly higher frequencies centred at 3280, 3324, 2846, 1705, 1683, 1081 and 1039 cm^{-1} , respectively, which corresponds to $-\text{NH}$, $-\text{OH}$, $-\text{CH}$ (alkanes), carbonyl and alkenes, respectively. The appreciable signal shift displayed by various functional groups of **BCG6a** is direct evidence of the participation of different functional groups in molecular assembly. The energy-minimised structure is obtained to elucidate the packing arrangement, and their molecular length is calculated and compared with experimental SAXRD diffraction data shown in Fig. 2c.

The xerogel obtained from **BCG6a** furnished 2θ at 2.21° , 3.37° , 8.72° , 20.81° , 22.59° and 40.80° , corresponding to interplanar d spacing values of 4.31, 2.62, 1.01, 0.43, 0.39, and 0.22 nm. The end-to-end molecular length of **BCG6a** obtained from computational studies is 3.01 nm, which is lower than the experimental value of 4.31 nm, suggesting the formation of an intercalated double layer stabilised by intermolecular hydrogen bonding (Fig. 2d).

A rheological measurement is performed to understand the practical utility of **BCG6a** hydrogel in pharmaceutical sectors (Fig. 3). Rheological measurements define the extent of deformation of the material from its original state in terms of storage modulus G' (elasticity) and loss modulus G'' (viscous) in response to strain. It was observed from the frequency sweep test that both the values of G' and G'' increase linearly in response to applied frequency; the higher value of G' compared to G'' reflects the strong tolerance of the gel in response to applied frequency. In the strain sweep test, it was observed that the storage modulus of the gel G' has higher values than the loss modulus G'' , reflecting the good mechanical strength of the gel. The thixotropy renders

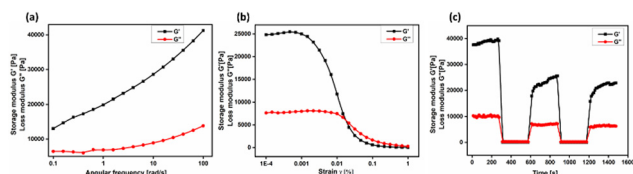


Fig. 3 (a) and (b) Angular frequency and strain amplitude dependence of G' and G'' of the hydrogel, and (c) thixotropy of the hydrogel formed by compound **BCG6a**.

fast structural recovery behaviour in response to the applied constant strain, an essential feature in medicine formulation.²⁴

To assess the feasibility of utilizing the compounds for anticancer studies, it is crucial to evaluate their cytotoxicity. The cytotoxicity of compound **BCG6a** on cellular metabolic activity was tested using immortalized human corneal epithelial cells (HCEC) treated with 500 μM of the compound. Cell viability and cytotoxicity were measured through an MTT assay, as shown in Fig. 4a. The results demonstrated that compound **BCG6a** exhibited almost 100% cell viability after a 6 h incubation and over 90% viability after 24 h.

Philawanol is known to exert significant anti-cancer activity and conversion into glycoconjugates is expected to enhance its potential. Hence, we investigated the anti-cancer activity of the synthesized glycolipids on the HeLa cells.²⁵ It is worth mentioning that low-molecular self-assembled systems play a prominent role in anti-cancer activity.²⁶ In the present studies, the anticancer potential of the chosen glycolipids was compared with 5-fluorouracil, which is sold under the name of Adrucil, a cytotoxic chemotherapy medication used to treat stomach cancer, oesophageal cancer, pancreatic cancer, breast cancer, and cervical cancer. The anti-cancer studies of 5-fluorouracil against the HeLa cells displayed an IC_{50} of 500 μM (Fig. 4b). For our investigation, we have selected **BCG5a**, which is an unsaturated version of **BCG6a**, and **BCG5b**, which is the c_4 epimer of **5a** and an unsaturated version of **BCG6b**, respectively Fig. 4(c)–(f).

The cytotoxicity of the compounds was examined by using an Alamar blue cell viability assay, which is generally used to quantitatively measure cell proliferation and cytotoxicity involving the oxidation–reduction process. We observed that **BCG6a** and **6b** exhibited a cytotoxic response, as shown in Fig. 4e–f after treatment for 24 h. The cellular morphology was also altered after the treatment as cells began to detach from the plate's surface, as illustrated in Fig. 5 for **BCG6a**, Fig. 6 for **BCG6b**, and for **BCG5a** and **BCG5b** in Fig. S50 and S51 (ESI[†]), respectively. In the case of compounds **BCG6a** and **BCG6b**, with increasing concentrations of both compounds, more cells detached from the surface and adopted a rounded appearance, indicating cell death. Interestingly, compounds **BCG6a** and **BCG6b** demonstrated significant activity,

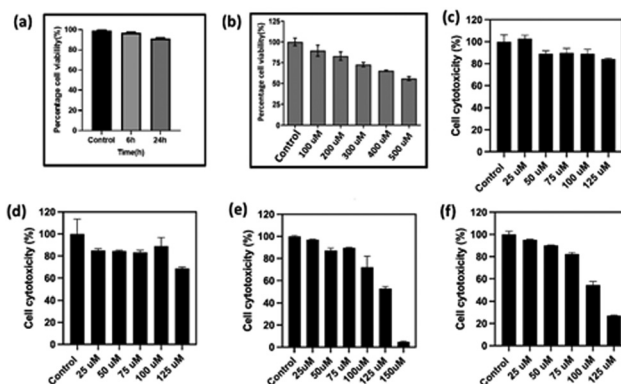


Fig. 4 (a) Cytotoxic assay of **BCG6a** on human corneal epithelial cells (HCEC), (b) anticancer assay of HeLa cells against 5-fluorouracil, (c)–(f) anti-cancer assay of HeLa cells after treatment with (c) **BCG5a**, (d) **BCG5b**, (e) **BCG6a**, and (f) **BCG6b** for 24 h. The values are represented as mean \pm S.E.M. for three values.



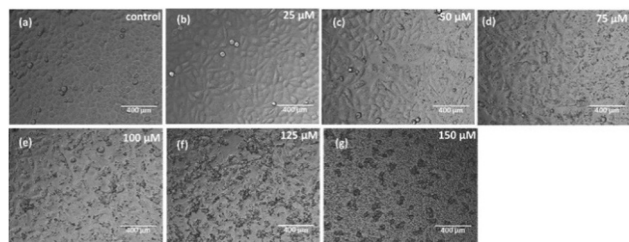


Fig. 5 (a)–(g) Microscopic images of the anticancer effect on HeLa cells of **BCG6a** at different concentrations at a magnification of 10 \times .

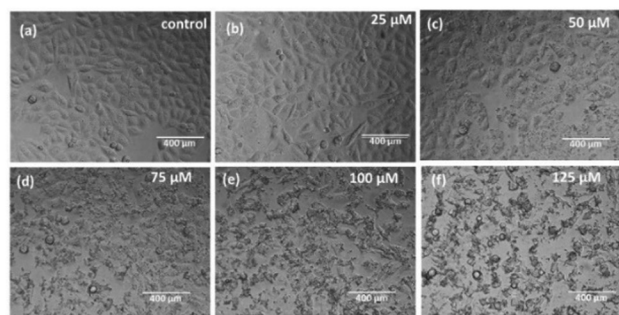


Fig. 6 (a)–(f) Microscopic images of the anticancer effect on HeLa cells of **BCG6b** at different concentrations at a magnification of 10 \times .

with IC₅₀ values of 125 μ M. This is a remarkable result compared to the standard 5-fluorouracil, which exhibits an IC₅₀ value of 500 μ M.

In conclusion, a new class of glycolipids were synthesised under environmentally friendly conditions from renewable resources in good yields. The bottom-up assembly of glycolipids generated hydrogel and oleogel, which were well characterized by NMR, IR, SEM, XRD, and rheological studies. Self-assembled **BCG6a** and **BCG6b** displayed anti-cancer activity toward HeLa cells at IC₅₀ of 125 μ M with minimal side effects broadening the application of supramolecular chemistry in medicine.

The manuscript was written through contributions of all authors. All authors have given approval to the final version of the manuscript.

The authors gratefully acknowledge the financial support from SERB (sanction order no. CRG/2023/002466) and DST FIST (SR/FST/CS-II/2018/65). The authors thank the National Institute of Technology Warangal for the infrastructure facilities.

Data availability

The data supporting this article have been included as part of the ESI.[†]

Conflicts of interest

There are no conflicts to declare.

Notes and references

- (a) P. Anand, A. B. Kunnumakara, C. Sundaram, K. B. Harikumar, S. T. Tharakan, O. S. Lai, B. Sung and B. B. Aggarwal, *Pharm. Res.*, 2008, **25**, 2097–2116; (b) D. S. Shewach and R. D. Kuchta, *Chem. Rev.*, 2009, **109**, 2859–2861; (c) S. Fu and X. Yang, *J. Mater. Chem. B*, 2023, **11**, 4584–4599.

- (a) N. Behtash and N. Mehrdad, *J. Cancer Prev.*, 2006, **7**, 683–686; (b) S. Feng, D. Lin, J. Lin, B. Li, Z. Huang, G. Chen, W. Zhang, L. Wang, J. Pan, R. Chen and H. Zeng, *Analyst*, 2013, **138**, 3967–3974; (c) P. L. Wantuch and F. Y. Avci, *Hum. Vaccines Immunother.*, 2018, **14**, 2303–2309.
- (a) B. Premalatha, *Indian J. Exp. Biol.*, 2000, **38**, 1177–1182; (b) M. Semalty, A. Semalty, A. Badola, G. P. Joshi and M. S. Rawat, *Pharmacogn. Rev.*, 2010, **4**, 88–94; (c) P. H. Gedam, P. S. Sampathkumaran and M. A. Sivasamban, *Phytochemistry*, 1974, **13**, 513–515; (d) Y. Qi, J. Lang, X. Zhu, J. Huang, L. Li and G. Yi, *RSC Adv.*, 2019, **10**, 1132–1141.
- (a) M. Semalty, A. Semalty, A. Badola, G. P. Joshi and M. S. M. Rawat, *Pharmacogn. Rev.*, 2010, 88–94; (b) Z. Qi, C. Wang and J. Jiang, *Molecules*, 2018, **23**, 1074; (c) T. K. Mohanta, J. K. Patra, S. K. Rath, D. K. Pal and H. N. Thatoi, *RES Essay*, 2007, **2**, 486–490.
- A. K. Mishra, A. Jain, C. Y. Jagtap, G. Dane, S. Paroha and P. K. Sahoo, *Fitoterapia*, 2024, **175**, 105978.
- (a) S. Mabic, C. Benezra and J. P. Lepoittevin, *Tetrahedron Lett.*, 1993, **34**, 4531–4534; (b) M. A. Elsohly, W. Gul, M. K. Ashfaq and S. P. Manly, WO/2009/146131, 2009.
- (a) J. Brand-Miller, J. McMillan-Price, K. Steinbeck and I. Caterson, *Asia Pac. J. Clin. Nutr.*, 2008, **17**, 16–19; (b) F. Yin, J.-J. Li, B. Shi, K. Zhang, X.-L. Li, K.-R. Wang and D.-S. Guo, *Mater. Chem. Front.*, 2023, **7**, 5263–5287.
- E. C. Calvaresi and P. J. Hergenrother, *Chem. Sci.*, 2013, **4**(6), 2319–2333.
- K. H. Tomaszowski, N. Hellmann and V. Ponath, *et al.*, *Sci. Rep.*, 2017, **7**, 13925.
- (a) D. Hanahan and R. A. Weinberg, *Cell*, 2011, **144**, 646–674; (b) E. Varghese, S. M. Samuel, A. Lišková, M. Samec, P. Kubatka and D. Büsselberg, *Cancers*, 2020, **12**, 1–34.
- Z. Wu, S. Chen, Z. Chen, G. Dong, D. Xu and C. Sheng, *J. Med. Chem.*, 2024, **67**, 7373–7384.
- K. C. Carvalho, I. W. Cunha, R. M. Rocha, F. R. Ayala, M. M. Cajiaba, M. D. Begnami, R. S. Vilela, G. R. Paiva, R. G. Andrade and F. A. Soares, *Clinics*, 2011, **66**, 965–972.
- (a) V. Di Bussolo, E. C. Calvaresi, C. Granchi, L. Del Bino, I. Frau, M. C. Dasso Lang, T. Tuccinardi, M. Macchia, A. Martinelli, P. J. Hergenrother and F. Minutolo, *RSC Adv.*, 2015, **5**, 19944–19954; (b) S. S. Mullapudi, D. Mitra, M. Li, E. T. Kang, E. Neoh and K. G. Chiong, *Mol. Syst. Des. Eng.*, 2020, **5**, 772–791; (c) H. Martin, L. R. Lázaro, T. Gunnlaugsson and E. M. Scanlan, *Chem. Soc. Rev.*, 2022, **51**, 9694–9716.
- L. Su, Y. Feng, K. Wei, X. Xu, R. Liu and G. Chen, *Chem. Rev.*, 2021, **121**, 10950–11029.
- S. I. Elshahawi, K. A. Shaaban, M. K. Kharel and J. S. Thorson, *Chem. Soc. Rev.*, 2015, **44**, 7591–7697.
- (a) F. Raza, H. Zafar, X. You, A. Khan and J. Wu, *Cancer Nanomed.*, 2019, 7639–7655; (b) F. Yin, J. J. Li, B. Shi, K. Zhang, X. L. Li, K. R. Wang and D. S. Guo, *Mater. Chem. Front.*, 2023, **7**, 5263–5287.
- P. Stallforth, B. Lepenies, A. Adibekian and P. H. Seeberger, *J. Med. Chem.*, 2009, **52**, 5561–5577.
- F. Hossain and P. R. Andreana, *Pharmaceuticals*, 2019, **12**, 84.
- (a) P. Jain and H. P. Sharma, *Int. J. Res. Pharm. Chem.*, 2013, **3**, 564–572; (b) P. K. Vemula and G. John, *Acc. Chem. Res.*, 2008, **41**, 769–782.
- A. K. Rachamalla, V. P. Rebaka, T. Banoo, R. Pawar, M. Faizan, K. Lalitha and S. Nagarajan, *Green Chem.*, 2022, **24**, 2451–2463.
- C. Fontana and G. Widmalm, *Chem. Rev.*, 2023, **123**, 1040–1102.
- (a) D. K. Smith, *Soft Matter*, 2023, **20**, 10–70; (b) M. Inès and G. Dhouha, *Carbohydrate Res.*, 2015, **416**, 59–69; (c) A. Thamizhanban, S. Balaji, K. Lalitha, Y. S. Prasad, R. V. Prasad, R. A. Kumar, C. U. Maheswari, V. Sridharan and S. Nagarajan, *J. Agric. Food Chem.*, 2020, **68**, 14896–14906.
- E. R. Draper and D. J. Adams, *Chem*, 2017, **3**, 390–410.
- A. R. Patel, M. Babaahmadi, A. Lesaffer and K. Dewettinck, *J. Agric. Food Chem.*, 2015, **63**, 4862–4869.
- (a) M. N. Mallick, W. Khan, M. Singh, M. Z. Najm, M. Kashif, S. Ahmad and S. Husain, *Drug Dev. Ther.*, 2016, **7**, 55; (b) R. K. Singh, B. Mallik, A. Ranjan, R. Tripathi, S. S. Verma, V. Sharma, S. C. Gupta and A. K. Singh, *Nat. Prod. Res.*, 2024, **38**, 1080–1084; (c) J. Fu, J. Yang, P. H. Seeberger and J. Yin, *Carbohydr. Res.*, 2020, **498**, 108195.
- (a) A. K. Das and P. K. Gavel, *Soft Matter*, 2020, **16**, 10065–10095; (b) Z. Yang, K. Xu, Z. Guo, Z. Guo and B. Xu, *Adv. Mater.*, 2007, **19**, 3152–3156; (c) W. Huang, J. Seo, S. B. Willingham, A. M. Czyzewski, M. L. Gonzalgo, I. L. Weissman and A. E. Barron, *PLoS One*, 2014, **9**, 1–10.

